Technical University of Varna Annual Journal
https://doi.org/10.29114/ajtuv.vol8.iss2.312
Vol. 8 Issue 2 (2024)
Published: 2024-10-01
ISSN 2603-316X (Online)

Investigation of tribological characteristics of 40X grade steel after hardfaced MMA welding method

Tatyana Mechkarova[a], *Apostol Ucherdzhiev*[a], *Nikolay Valchev*[a], *Desislava Mincheva*[a].

[a] Faculty of Manufacturing Engineering and Technologies, Technical University of Varna, Bulgaria

Corresponding author contact: t.mechkarova@tu-varna.bg

Abstract. *The article discusses the selection of an appropriate technology for the repair of forged structural steel through the use of hardfacing MMA welding method. Investigated, additionally, is the wear resistance of the hardfacing layers. The method used to determine the wear resistance is "block on ring". The macrostructure, microstructure and Vickers microhardness (HV0.05) were also analyzed.*

Keywords: hardfacing, MMA welding method , wear, macrostructure, microstructure, microhardness, block on ring

1 Introduction

Basic compressors used in ship equipment are large and expensive equipment, whose replacement in case of failure would require a significant investment of resources and time (Denev, Y., 2022). It is, therefore, more practical to repair the defective parts in order to save time and money. The components most scusceptible to defects are typically those that experience wear due to friction or overload, such as crankshafts, connecting rods, pistons, and bearings. Technologies for their repair most often involve surfacing welding followed by precision machining with metal cutting tools.

The wear process (including abrasive, adhesive, and fatigue wear) is complex (G. V. Duncheva, 2022). Various tests and methods have been developed to simulate the wear mechanisms, and yet there is no universally accepted method for establishing specific wear parameters (Lyutskanov, K., 2018). Typically, wear measurements determine the extent of weight loss, width reduction, or depth erosion in the affected areas.

The objective of the research is to identify a technological solution to address the long-term problem of heavily loaded rotary elements in ship systems that are prone to wear.

The tasks to be solved are: developing a suitable methodology for repairing wear-resistant layers through hardfacing and researching their resistance to wear

2 MATERIALS AND METHODS

2.1 Material and specimen preparation

For the purposes of the present study, two specimens of 40X steel (according to GOST 4543 standard) were prepared using a turning method (Fig. 1-a). The material of the specimens and the defective shaft is similar, with their geometrical dimensions outlined in Fig. 1-b. The chemical composition of the 40X steel used is shown in Table 1.

During operation, the shafts are twisted, necessitating a tough core. To achieve this, thermal softening of the speciments material was carried out.

Fig. 2 shows a cyclogram of the performed heat treatment (Haivoronskyi, O. A., 2016).

Technical University of Varna
Annual Journal
https://doi.org/10.29114/ajtuv.vol8.iss2.312
Vol. 8 Issue 2 (2024)
Published: 2024-10-01
ISSN 2603-316X (Online)

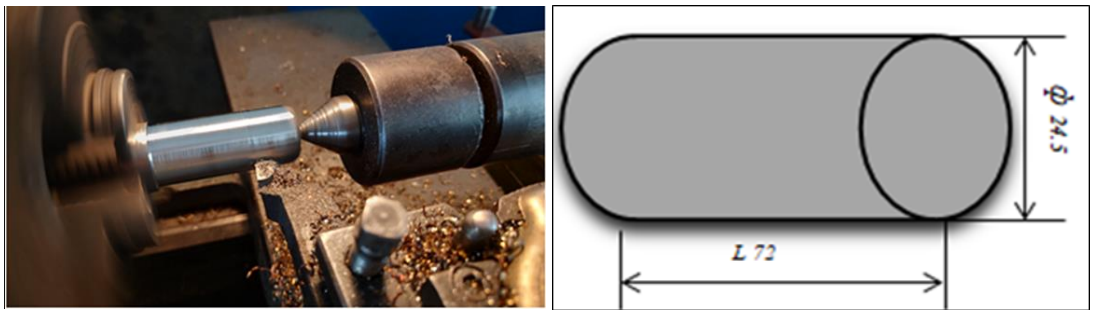

а б

Fig. 1. Shape and dimensions of test specimens.

Table 1. Chemical composition in percentages of steel 40X.

C	Si	Mn	Ni	Cr	Cu	P	S
0.36-0.41	0.17-0.37	0.5-0.8	≤0.3	0.8-1.1	≤0.3	≤0.035	≤0.035

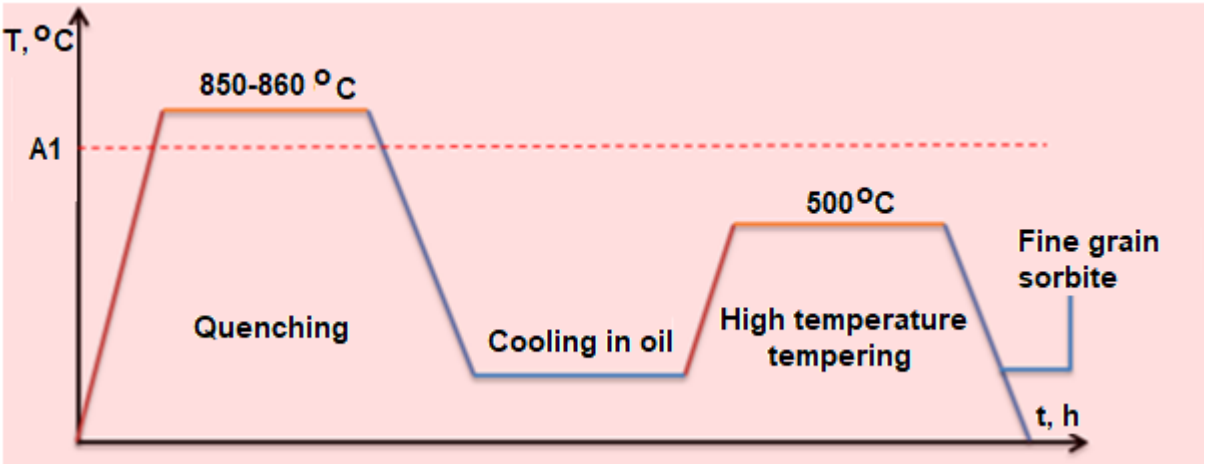

Fig. 2. Cyclogram of heat treatment of specimens.

For the correct welding of the cylindrical specimens, a specialized stand was constructed (Fig. 3). The stand is equipped to measure thermal deformations.

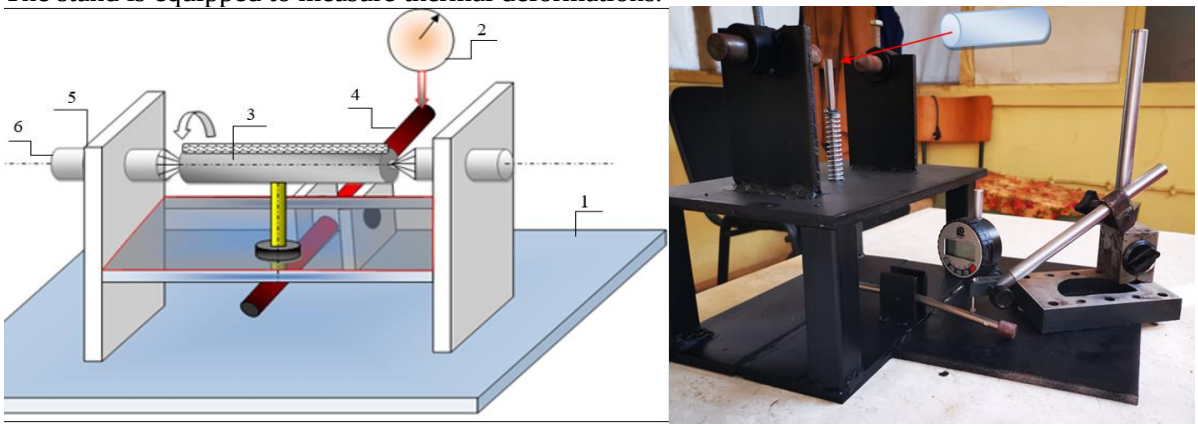

Fig. 3. Stand for surfacing welding:
1. Base; 2. Indicator clock; 3. Specimen; 4. Lever; 5. Columns; 6. Centerpunch

Technical University of Varna
Annual Journal
https://doi.org/10.29114/ajtuv.vol8.iss2.312
Vol. 8 Issue 2 (2024)
Published: 2024-10-01
ISSN 2603-316X (Online)

Fig. 4. Sequence of applying the welded layers

Surfacing welding was performed by two methods (Shravan, 2023) with electrodes presented in Table 2.

Table 2. Chemical composition in percentages of the selected brands of electrodes from the company ESAB.

	C	Si	Mn	Ni	Cr
OK84.42	0.12	0.5	0.3	-	13.0
OK61.20	0.02	0.4	1.9	9.8	19.8

The first sample was preheated in an electric resistance furnace to a temperature calculated according to the carbon equivalent of 200◦C and then surface welded with an OK84.42 electrode using the MMA welding method.

The pre-heating of the steel is done in order to prevent the formation of cold cracks in the welded layers (Lingamanaik, 2014) with electrode brand OK84.42. According to ESAB's technical data sheet, this electrode provides excellent wear resistance to the welded layers.

The second sample underwent no preheating, but a buffer layer (Denev, Y. S., 2023) was welded using an OK 61.20 electrode, and then completed with surface welding with the electrode brand OK 84.42. The buffer electrode is an austenitic grade of steel and has a lower hardness than the OK84.42 electrode.

Subsequently, microstructures were created from the samples to study their macro and micro structure, as well as to assess their wear resistance.

In order to conduct a more accurate study of wear in the operating conditions of shafts (Bankova, A., 2022) and axes in contact with sliding bearings, an experimental investigation of the tribosystem "CuAl8Fe3 - steel 40X" was carried out with the use of the kinematic scheme " block on ring " (Fig. 5).

The schematic diagram of the experimental setup for the wear tests is illustrated in Fig.6. The test specimen (segment) is fixed in the bed of a specially designed holder within the loading beam. The inner cylindrical surface of the segment comes into contact with the surface of a rotating sample held in the chuck, rotatig at a constant frequency of1400 min-1. The normal load F is applied at the center of gravity of the contact area between the specimen and the counter body, and is set by a lever system in the loading beam. The tests were conducted under the same conditions for all samples in dry friction mode.

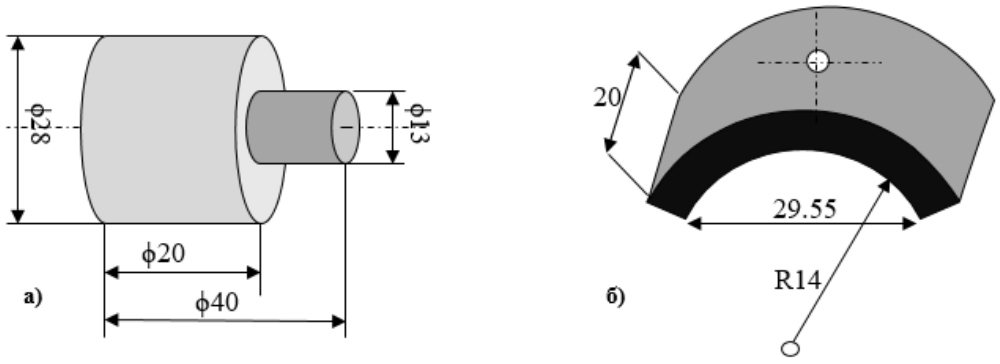

Fig. 5. Shape and dimensions of: a) test sample; b) counter body

Technical University of Varna
Annual Journal
https://doi.org/10.29114/ajtuv.vol8.iss2.312
Vol. 8 Issue 2 (2024)
Published: 2024-10-01
ISSN 2603-316X (Online)

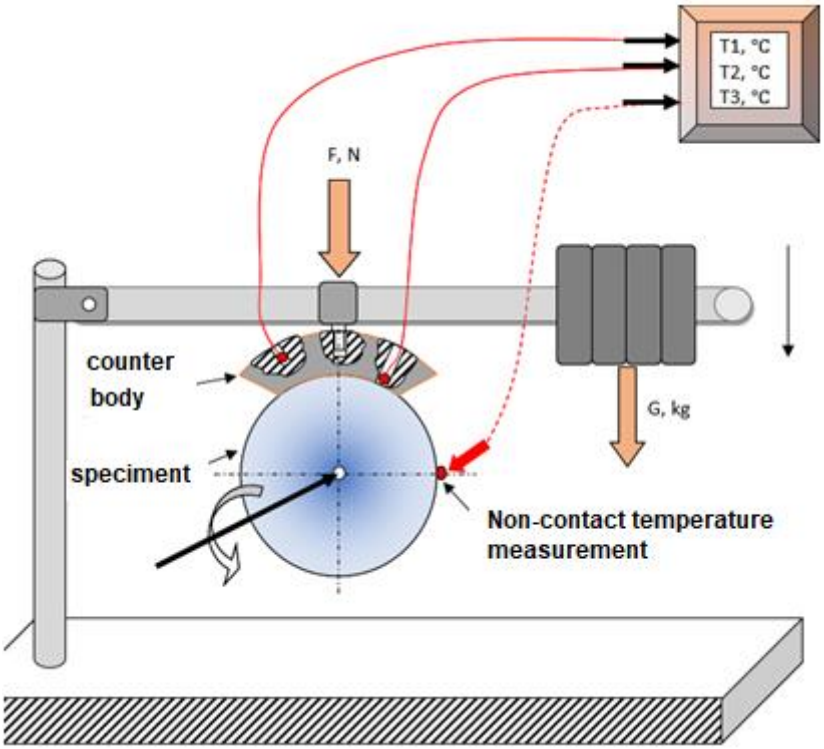

Fig. 6. Wear test stand

For the correct determination of wear, it is essential to calculate the contact area - S, [mm2] between the test specimen and the counterbody, the normal load - F, [N] path-L, [m], and the pressure – $\wp$, [MPa], as shown in Fig. 7.

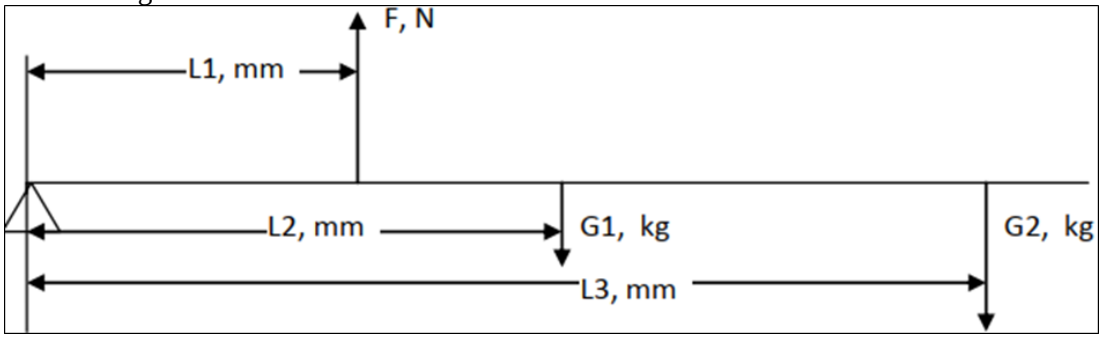

Fig. 7. Load diagram

Technical University of Varna Annual Journal
https://doi.org/10.29114/ajtuv.vol8.iss2.312
Vol. 8 Issue 2 (2024)
Published: 2024-10-01
ISSN 2603-316X (Online)

S=L (in an arc) x L (length) = 29,55x20=591[mm^2]; (1)

G2=π.τ^2. L (lever). 7.86 = 0,187[kg]; (2)

G1. L2 + G2. L3 - F.L1= 0; (3)

F.L1= G1. L2 + G2. L3= 0,187. 106+0,510. 152 = 97,34 [$\frac{kg}{m}$]; (4)

F = $\frac{97,34}{22}$[$\frac{kg}{m}$]; F = 4,42kg; F =44,2[N] (5)

$\mathcal{p}$= $\frac{44,2}{591}$ = 0,074[MPa] (6)

L (path) =94[mm] x1400[min^{-1}] =131600 mm, for one minute; =131,6[m] for one minute. (7)

L (sample)= π.D=π.30=94 [mm]; (8)

for 10 [min] =1316 [m] → 1,316 [km]. (9)

To determine the wear resistance, the mass wear of the specimens and the corresponding temperature at specific path distances and friction time are measured, under constant preset conditions of load and sliding speed. Based on the mass wear data, the corresponding wear resistance characteristics are then calculated.

The methodology includes the following sequence: Measurement of the mass of the specimen before friction using "KERN PCB" electronic scales with an accuracy of 0.001 g. Prior to each mass measurement, the specimen is cleaned of any mechanical and organic particles, and dried with ethyl alcohol to prevent the electrostatic effect.

After a designated friction path, the mass of the specimen m1 is measured, and the following wear characteristics are calculated. Mass wear Δm is determined as the difference between the mass of the specimen before friction m0 and that after a certain path/time of friction m1 : Δm = m0 – m1.

During the test, temperature measurements were taken on the specimen, counterbody, and non-contact areas of the specimen.

3 RESULTS

3.1 Macrostructural analysis

Displayed in Fig. 8 are two macrostructural images of specimens 1 and 2 of steel 40X (Fig. 7). Specimen 1 is preheated to 200°C and then surface welded with electrode OK 84.42, while specimen 2 is not preheated, but has a surface welded buffer layer of electrode OK 61.20, and on the top is surface welded with electrode OK 84.42.

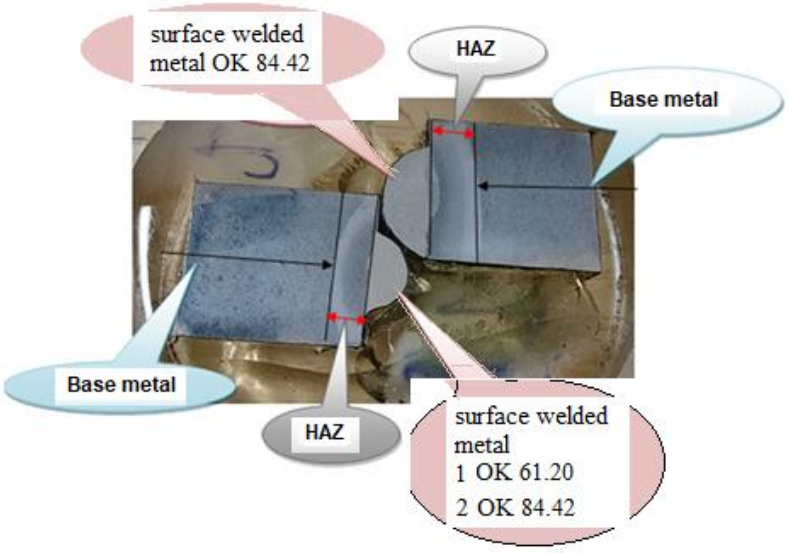

Fig. 7. Macrostructure of experimental specimens

Technical University of Varna
Annual Journal
https://doi.org/10.29114/ajtuv.vol8.iss2.312
Vol. 8 Issue 2 (2024)
Published: 2024-10-01
ISSN 2603-316X (Online)

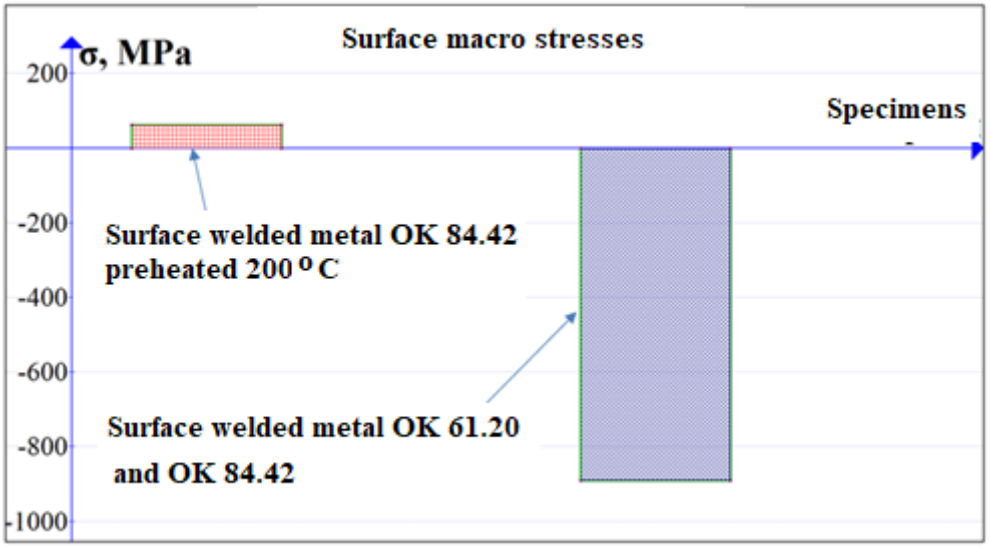

Fig. 7. Measured macro stresses in the test surface welded specimens with an X-ray diffractometer

The tensile stresses of the preheated and surface welded metal are significantly below the strength limits Rm and the yield strength Re, which gives us reason to consider that there is no risk of cold cracks occurrences across the surface of the welded layer.

The test specimen preheated to 200℃ and then surface welded with an OK 84.42 electrode, shows low tensile stresses of 63.28 [MPa]. The test specimen surface welded with a buffer layer of electrode 61.20 and then with electrode OK 84.42 on top exhibits no tensile but compressive stresses of 850[MPa].

Both welding methods yielded excellent results.

3.2 Microstructural analysis

According to the selected technological process (with pre-heating and subsequent welding with OK 84.42 electrode) on specimen 1, the following areas of the microstructures become visible in Fig.8 .

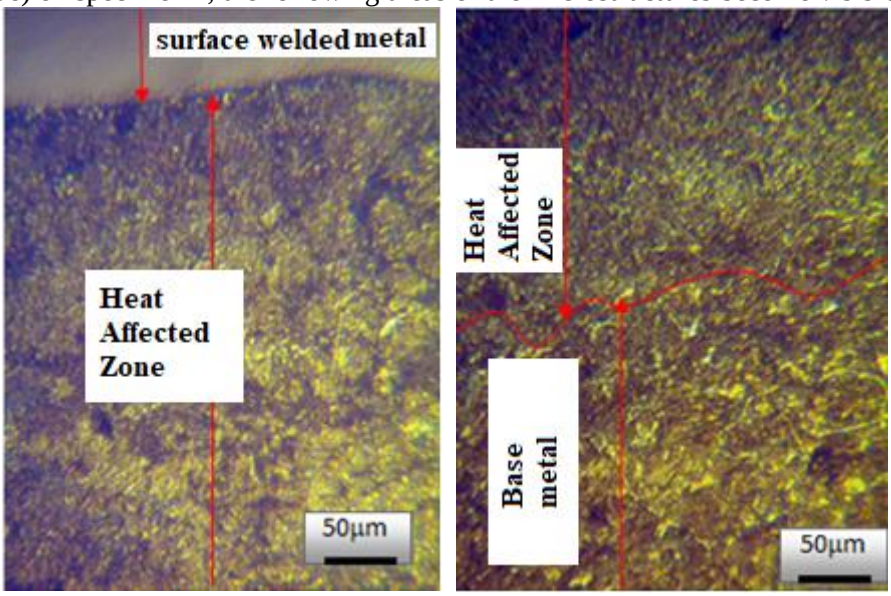

Fig. 8. Microstructures of specimen 1 with X100 magnification

Technical University of Varna
Annual Journal
https://doi.org/10.29114/ajtuv.vol8.iss2.312
Vol. 8 Issue 2 (2024)
Published: 2024-10-01
ISSN 2603-316X (Online)

Fig. 9 shows the microstructures of specimen 2 without pre-heating and with a buffer layer OK 61.20.

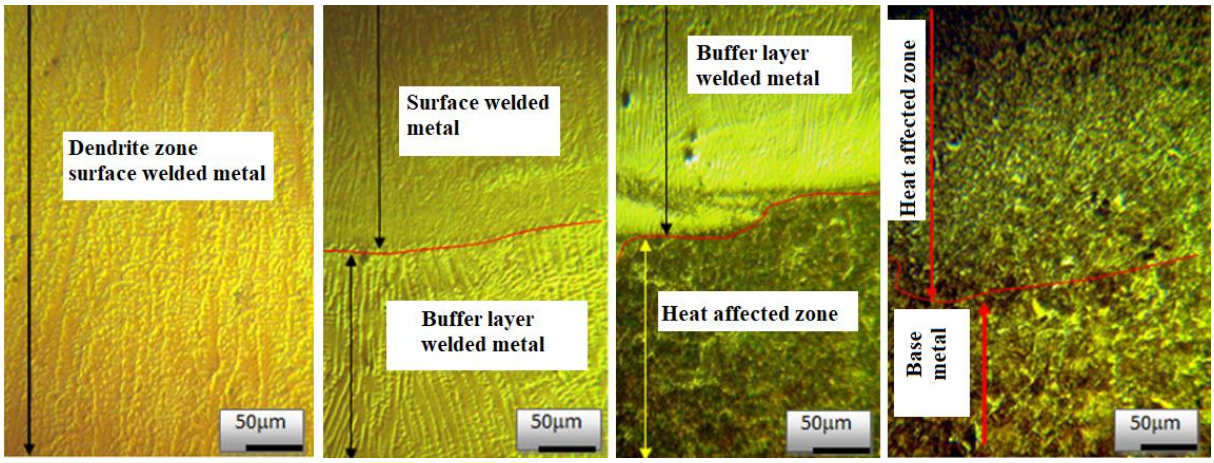

Fig. 9. Microstructures of specimen 2 with X100 magnification

The microstructures (Fig. 8 and Fig. 9) indicate that the wider heat affected zone (HAZ) can be seen in the sample without a buffer layer. The smaller HAZ in sample 2 is probably caused by the poor thermal conductivity of the stainless steel buffer layer

3.3 Results for measured microhardnesses

A Vickers microhardness test was performed to determine the hardening of the test specimens. The results of the study are graphically represented in Fig. 10.

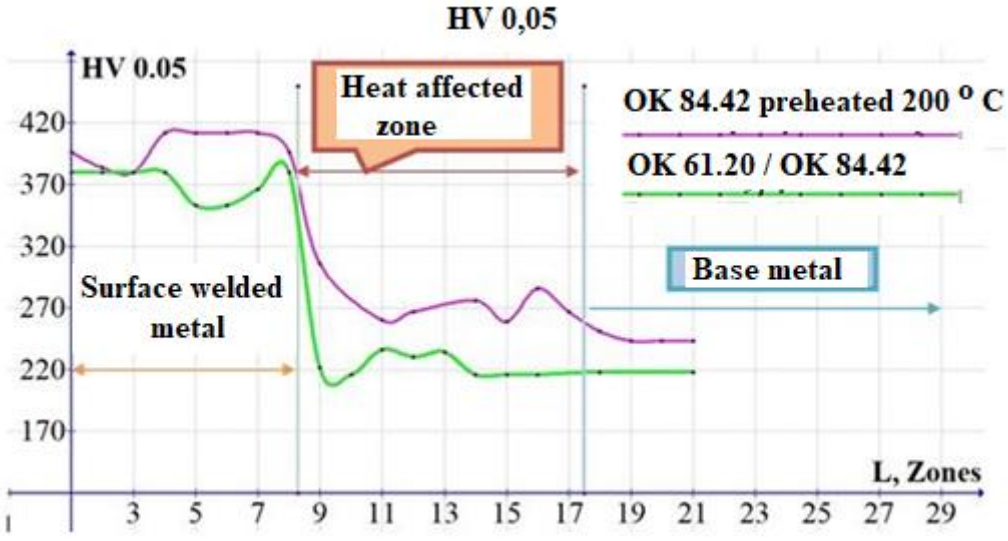

Fig. 10. Microhardness HV 0,05

The graph in Fig.10 shows that we have higher micro-hardness values in the surface layer and head affected zone of speciment 1, which is likely due to the chemical composition of the electrode OK84.42.

Technical University of Varna
Annual Journal
https://doi.org/10.29114/ajtuv.vol8.iss2.312
Vol. 8 Issue 2 (2024)
Published: 2024-10-01
ISSN 2603-316X (Online)

3.4 Results for weight loss in dry friction mode.

Upon the weight measurements of the metal loss from the welded layers, the graphic lines in Fig.11 were constructed to visually depict the lower wear resistance of specimen 2 (hardfaced with a buffer layer).

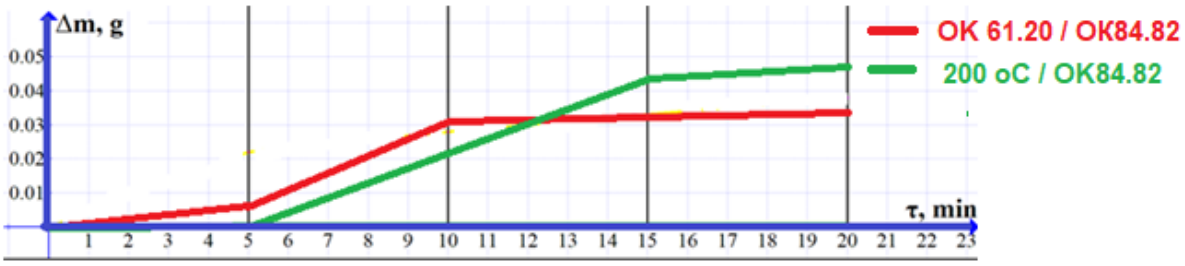

Fig. 11. Weight loss of experimental specimens

For specimen 2 with a buffer layer, the measured wear is less due to the formation of deposits during friction with the counter body.

This, however, does not allow us to obtain the necessary wear accuracy at this stage.

4 Conclusions

A stand for surface welding cylindrical specimens has been developed, giving the possibility to measure the deformations during welding.

The macrostrains measured with the X-ray diffractometer are below the yield strength of the base metal, with negligible tensile stresses of +62 MPa. The compressive stresses in test specimen 2 with applied buffer layer, are significantly higher than those in test specimen 1, indicating a high fatigue strength.

It was observed that the thickness of the heat affected zone in buffer layer of the specimen 2 was significantly narrower and finer grained compared to specimen 1.

The hardness tests revealed that both specimens exhibit a hardness level fluctuating around 450 HV during research surface welding processes, indicative of good results in the repair of bearing necks.

Surface welding with a buffer layer has better technological parameters, maintaining hardness during welding and producing a narrower heat affected zone (suitable conditions for fatigue strength).

The dry wear tests confirmed that the specimen with applied buffer layer (specimen 2) outperforms the preheated specimen 1.

References

Denev, Y. (2022). Application of hardfacing arc methods in Bulgarian ship repair SME. Trans Motauto World, 7(2), (pp.50-52).

Lyutskanov, K. (2018). Analysis and optimization of hydroabrasive wear of surfacing layers fomred by using the method of gas-thermal welding with metal powders alloys. *SCNVNA, 32,* (pp.62-65). https://doi.org/10.14748/scnvna.v32i0.4498.

Denev, Y. S., Rafetova, A., & Dichev, P. (2023). Study into the process of defective railtrack arc-hard-facing. *Annual Journal of Technical University of Varna, Bulgaria, 7(1),* (pp.33-43). https://doi.org/10.29114/ajtuv.vol7.iss1.281.

ESAB (n.d). Catalog of ESAB electrodes. Retrieved from: https://esab.com/gb/eur_en/

Bankova, A. (2022). Investigation of the Qualitative Dependence between the Character of Wear and the Mutual Location of Wearing Supports. *In 2022 International Conference on*

https://doi.org/10.29114/ajtuv.vol8.iss2.312
Vol. 8 Issue 2 (2024)
Published: 2024-10-01
ISSN 2603-316X (Online)

Communications, Information, Electronic and Energy Systems (CIEES), 1-4. IEEE. https://doi.org/10.1109/CIEES55704.2022.9990870

Lyutskanov, K., Hristov, H., & Demirova, K. (2018). Experimental research of abrasive wear of surfacing layers. *SCNVNA, 32,* (pp.52-56). https://doi.org/10.14748/scnvna.v32i0.4496.

G. V. Duncheva, J. T. Maximov, A. P.Anchev, V. P. Dunchev, Y. B. Argirov,and M. Kandeva-Ivanova, (2022), "Enhancement of the wear resistance of CuAl9Fe4 sliding bearing bushings via diamond burnishing," *Wear, vol. 510–511,* (p. 204491), https://doi.org/10.1016/j.wear.2022.204491.

Haivoronskyi, O. A., Poznyakov, V. D., Markashova, L. I., Ostash, O. P., Kulyk, V. V., Alekseenko, T. O., & Shyshkevych, O. S. (2016). Structure and mechanical properties of the heat-affected zone of restored railway wheels. Materials Science, 51, (pp.563-569), https://link.springer.com/article/10.1007/s11003-016-9876-6

S. N. Lingamanaik and B. K. Chen, (2014), "Microstructural and thermomechanical analysis of quench cracking during the production of bainitic-martensitic railway wheels," Eng. Fail. Anal., 40, (pp.25–32), Retrieved from: https://www.sciencedirect.com/science/article/pii/S1350630714000442

Shravan C,N. Radhika Icon,N. H. Deepak Kumar &B. Sivasailam, (2023), A review on welding techniques: properties, characterisations and engineering applications, Advances in Materials and Processing Technologies, https://doi.org/10.1080/2374068X.2023.2186638